Clim. Past Discuss., doi:10.5194/cp-2016-6, 2016
Manuscript under review for journal Clim. Past
Published: 3 February 2016

Climate of the Past Discussions
Open Access
EGU

A 368-year maximum temperature reconstruction based on tree ring data in northwest Sichuan Plateau (NWSP), China

Liangjun Zhu[1], Yuandong Zhang[2], Zongshan Li[3], Binde Guo[1], Xiaochun Wang[1]

[1] Center for Ecological Research, Northeast Forestry University, Harbin 150040, China
[2] Key Lab of Forest Ecology and Environment, State Forestry Administration, Institute of Forest Ecology, Environment and Protection, Chinese Academy of Forestry, Beijing 100091, China
[3] State Key Laboratory of Urban and Regional Ecology, Research Center for Eco-Environmental Science, Chinese Academy of Sciences, Beijing 100085, China

Correspondence to: Xiaochun Wang (wangxc-cf@nefu.edu.cn), Yuandong Zhang (zydxju@163.com)

Abstract. We present a reconstruction of July-August mean maximum temperature variability for northern West Sichuan Plateau (NWSP), China based on a chronology of tree-ring widths over the period 1646-2013 AD. A regression model explains 37.1 % of the variance of July–August mean maximum temperature during the calibration period from 1954 to 2012. Seven major cold periods were identified including 1708–1711, 1765–1769, 1818–1821, 1824–1828, 1832–1836, 1839-1842 and 1869–1877, and three major warm periods occurred between 1655–1668, 1719–1730 and 1858–1859 in our reconstruction. Comparison with other nearby temperature reconstructions and spatial correlations with gridded land surface temperature dates revealed that our temperature reconstruction has high spatial representativeness. 20th century rapid warming wasn't obvious in the NWSP mean maximum temperature reconstruction, which implied that mean maximum temperature might play an important and different role in global change as unique temperature indicators. Multi-taper method (MTM) spectral analysis revealed significant periodicities of 170-, 49-114-, 25–32-, 5.7-, 4.6–4.7-, 3.0–3.1-, 2.5- and 2.1–2.3-year quasi-cycles at a 95% confidence level. The mean maximum temperature variability in northwest Sichuan may be affected by ENSO, PDO, AMO and solar activity.

Keywords Temperature reconstruction; West Sichuan Plateau; *Picea purpurea*; Climate change; Tree-rings

1 Introduction

Northwest Sichuan Plateau (NWSP), located between the body of the Tibetan Plateau and the Sichuan Basin, is the transition zone of the Tibetan Plateau and the second step of China, which is one of the most sensitive and vulnerable areas to climate change (IPCC, 2013). Frequent temperature-related natural disasters, especially in summer (e.g., hailstones, frost damage), have a major influence on the natural ecosystem and human activities over the entire NWSP areas (Ma, 2006;Zheng and Yao, 2004). The climate of NWSP is complexly influenced by large-scale atmospheric circulation patterns, such as the Asian monsoon and the El-Niño/Southern Oscillation (ENSO), Atlantic Multidecadal Oscillation (AMO) and Pacific Decadal

Clim. Past Discuss., doi:10.5194/cp-2016-6, 2016
Manuscript under review for journal Clim. Past
Published: 3 February 2016

Oscillation (PDO) (Shao and Fan, 1999;Yu et al., 2012;Xiao et al., 2013;Qin et al., 2008;Song et al., 2007;Wu et al., 2005;Xiao et al., 2015;Deng et al., 2014;Duan et al., 2010), but driving mechanisms are not fully known or understood.

Long temperature records of NWSP are particularly critical for us to understand the variability of past temperature variations and the influences of large-scale atmospheric circulations as well as possible forcing mechanisms in order to predict future climate (Li et al., 2011;Thapa et al., 2014;Liang et al., 2008). Therefore, it is essential to explore long-term temperature variability from model-validated climate proxy data. However, most instrumental meteorological records from NWSP are of short length, covering only the past 40–60 years, and thus provide little information on climate variability over decades and longer.

Natural proxies, such as ice cores, speleothems, pollens, lake sediments, tree rings and so on, have the potential to fulfill this task (IPCC, 2013). Tree-ring data, a major proxy for paleoclimate research, have been widely used to reconstruct past climate worldwide (Gou et al., 2008;Deng et al., 2014;Wang et al., 2015;Thapa et al., 2014;Bräuning and Mantwill, 2004;D'Arrigo et al., 1998;Briffa et al., 1995) due to accurate dating, wide distribution, high resolution, and good replication (Stokes and Smiley, 1968;Fritts, 1976). In recent years, rapid progress in dendroclimatic reconstructions has occurred throughout China (Zhang, 2015). Among these reconstructions, only a few occurred in NWSP. Unfortunately, most of them were during a single month in summer or continuous months in winter, and most of them measured mean or minimum temperature rather than mean maximum temperature (Shao and Fan, 1999;Yu et al., 2012;Xiao et al., 2013;Qin et al., 2008;Song et al., 2007;Wu et al., 2005;Xiao et al., 2015;Deng et al., 2014;Duan et al., 2010).

Global warming already has been regarded as an indisputable fact (IPCC, 2013). Recent studies suggest that global warming has occurred mainly in the minimum temperatures and at night in most regions of the Northern Hemisphere, however, evidence of warming trends of maximum temperatures were not evident; variations of the mean, minimum, and maximum temperatures were asymmetric during the warming processes. It is suggested that we should focus more attention on reconstructing various temperature variables (e.g. maximum and minimum temperatures, etc.) but not the mean temperature (Wilson and Luckman, 2002;Wilson and Luckman, 2003). The aims of the present study are to (1) develop new tree-ring width chronologies for the timberline forests in NWSP; (2) reconstruct past mean maximum variations in late summer using the tree-ring chronology; (3) analyze and compare the new reconstruction with the existing reconstruction and historical data archives for NWSP; and (4) identify possible driver mechanisms of late summer temperature.

2 Materials and methods

2.1 Study area

Samples were collected from spruce (*Picea purpurea*) growing at the timberline forest of Ayila mountain in Chali township, located in NWSP (32°43′49″ N, 102°06′17″ E; 3900 m above sea level (a.s.l.)). This region is classified as a sub-humid climate type, and strongly influenced by the Asian monsoon, with dry periods from November to April and wet periods from May to October (Sherman et al. 2008). Based on records from the two nearest weather stations in Aba (1955-1990) and Hongyuan

Clim. Past Discuss., doi:10.5194/cp-2016-6, 2016
Manuscript under review for journal Clim. Past
Published: 3 February 2016

(1962-2013), the mean annual temperatures are 3.4 ℃ and 1.5 ℃, the mean monthly minimum temperatures are -5.4 ℃ and −2.9 ℃, and the mean monthly maximum temperatures are 10.2 ℃ and 12.2 ℃ (Table 1). The regional average annual precipitation ranges from 500 to 1000 mm, is highly variable on inter-annual timescales, and falls predominantly during the summer monsoon season (May to October, 86 %-89% ; Fig. 1).

The dark coniferous forests in this area are distributed within narrow bands on both sides of the valley and generally reach an altitude of 3500–4,000 m above sea level (a.s.l.). *P. purpurea* is the most widespread and dominant species with 80% coverage, mainly growing on typical mountain brown dark coniferous forest soils (according to the Chinese Soil Taxonomic System) (Li, 1995;Yang et al., 1992). As a shallow-root tree specie, *P. purpurea* is able to endure shade and humid conditions in addition to extreme cold, so that it usually grows at high altitudes where only a thin soil layer is covering the bedrock. The vegetation of this area is sub-alpine dark coniferous forests dominated by spruce, fir and cypress forests as well as some pines, birch and oaks, at low altitudes (Yang et al., 1992).

2.2 Tree-ring data

In July 2014, a total of 36 increment cores from 16 live trees were collected on opposite sides using an 5-mm diameter increment at breast height (above ground level 1.3 m) to avoid or reduce errors in different sides caused by topography, competition, climate and growth characteristic. In order to remove the influence of identifiable stand disturbances (including animal and human disturbance, windstorm, snow and fire damage) and any obvious abnormal growth, each sample tree and sampling area were selected carefully. According to standard dendrochronological procedures (Cook and Kairiukstis, 1990;Fritts, 1976), all cores were fixed by trogue and air dried at room temperature for 2–3 days in the laboratory. Afterwards, we progressively sanded those cores to a fine polish until individual tracheids within the annual rings were visible. Then, cross dating was performed to assign calendar years to each growth ring and identify possible false or absent rings using a Skeleton-plot cross-dating method (Stokes and Smiley, 1968), and subsequently tree-ring width was measured at 0.001 mm resolution using a semi-automatic Velmex tree ring measurement system (Velmex, Inc., Bloomfield, NY, USA). Cross-dating and measurement accuracy were checked both first visually and then statistically using the COFECHA computer program (Holmes, 1983). To remove the non-climate signals related to tree age or the effects of stand dynamics, cross-dated ring widths were detrended and standardized by fitting a conservative negative exponential curve or linear curve with negative slope using the ARSTAN program (Cook, 1985). We calculated ring width indices for each specimen by dividing the ring-width value by the value of the fitted curve for each year. The resulting ring-width indices were averaged together to generate a standard STD chronology for collection site (Cook, 1985).

The quality of the composite tree-ring chronology was evaluated estimating the mean correlation between series (RBAR) and expressed population signal (EPS). The RBAR provides an indication of chronology signal strength (common variance between all series) and is independent of sample size (Wigley et al., 1984), whereas the EPS assesses the degree to which the chronology represents a hypothetical chronology based on an infinite number of cores and is calculated from between-tree

Clim. Past Discuss., doi:10.5194/cp-2016-6, 2016
Manuscript under review for journal Clim. Past
Published: 3 February 2016

correlation and number of trees included in the calculation (Briffa et al., 1995). Running RBAR and EPS statistics were calculated for 51- year intervals of the chronology with 25-year overlaps to assess the stability of signal strength as chronology replication diminished back in time. In general, EPS using a threshold value of 0.85 was applied to assess the trusted starting year of the chronology (Wigley et al., 1984). Consequently, we only consider here the outer 368-year period, CE 1664–2012, of the reconstruction and analysis in this paper.

2.3 Climate and statistical analyses

Instrumental climatic data for our study, provided by the China Meteorological Data Sharing Service System (http://cdc.cma.gov.cn/), were available from the weather stations of Hongyuan (32°48′ N, 102°33′ E; 3248 m a.s.l.) and Aba (32°54′ N, 1101°41′ E; 3254 m a.s.l.). They are the two nearest stations to the tree-ring sampling sites of Chali with a maximum distance of about 42 km (Table 1). With similar seasonal rainfall distribution and climatic conditions, Hongyuan and Aba meteorological stations cover the period 1961–2013 and 1955–1990 of instrumental data, respectively (Fig. 1). Large-scale climate data (Atlantic Multidecadal Oscillation, AMO; Pacific Decadal Oscillation, PDO; Multivariate ENSO Index, MEI) were downloaded from the the KNMI climate explorer (http://climexp.knmi/nl).

In order to determine the relationship between tree growth and climate factors, the initial observed climatic data (total precipitations, mean, minimum, and maximum temperatures) from the previous July to current September of the two stations were used to perform a correlation analysis. Based on stronger relationship between the tree-ring index and previous July to August mean maximum temperature of Hongyuan and Aba, we reconstructed regional late summer (from July to August) mean maximum temperature (hereafter RLST) using a simple linear regression model. In order to obtain a long calibration/verification period of July-August mean maximum temperatures, the July and August mean maximum temperature of two stations were extended to the period 1955-2013 using linear regression of records from Hongyuan and Aba stations before reconstruction. Models explain 87 % of the variance in mean maximum temperature of July (correlation 0.93) and 92 % of the variance of August (correlation 0.96), which indicates that variations in temperature with time during the overlapping period have been very similar throughout the region.

A traditional split-period calibration/verification method was used to explore the temporal stability and reliability of the reconstruction model (Cook and Kairiukstis, 1990;Fritts, 1976). Multiple statistical parameters, including Pearson's correlation coefficient (r), the R square (R^2), the Sign test (ST), the reduction of error test (RE), coefficient of efficiency (CE), the product means test (PMT), the Durbin-Watson (DW) and the root mean square error (RMSE), were used to evaluate model ability of this method (Cook and Kairiukstis, 1990;Fritts, 1976). To examine the temporal and spatial representativeness of the temperature reconstruction, spatial correlation between actual and reconstructed RLST variables from this study and gridded (0.5°×0.5°) temperature data from 1955 to 2012 (CRU TS3.22 Maximum Temperature, Harris et al., 2014) were performed using the KNMI climate explorer (http://climexp.knmi/nl). We also compared our RLST reconstruction for the past 368 years with other tree-ring-based temperature reconstructions from nearby areas and over a large scale. A spectral analysis was

Clim. Past Discuss., doi:10.5194/cp-2016-6, 2016
Manuscript under review for journal Clim. Past
Published: 3 February 2016

performed to identify the periodicity of local climate variability reconstructed in this study using Multi-taper method (MTM) program (Mann and Lees, 1996).

3 Results

3.1 Tree growth–climate relationships

We used simple correlation analysis to identify climate signals in ring-width chronology using SPSS software. Relationships between the chronology of Chali and the Hongyuan and Aba monthly climate data were shown in Figure 4. A significant positive correlation ($p < 0.05$) between tree radial-growth of *P. purpurea* and mean and maximum temperature in the previous July and August was found at both of the weather stations, which indicated that the late summer mean maximum temperature in the previous year played a vital role for radial growth of *P. purpurea*. Ring-width chronology of *P. purpurea* was negatively ($p < 0.05$) associated with previous November mean and minimum temperature at the Hongyuan weather station, and a similar negative correlation relationship was also found at the Aba weather station, though not at a significant level. There was a significant negative correlation ($p < 0.05$) between tree radial-growth of *P. purpurea* and mean minimum temperature in June found at the Hongyuan weather station, however it was not significant at the Aba weather stations. The correlations between monthly precipitation data and the ring-width index were not significant at both weather stations. Therefore, we selected July-August mean maximum temperature as the target of our reconstruction.

3.2 Regional temperature reconstruction

We tried to reconstruct RLST history based on the strong relationship between previous July and August mean maximum temperature and tree-ring index. A simple linear regression model between TRI and the composite July-August mean maximum temperature of Hongyuan and Aba weather stations covering form 1955 to 2013 was created to reconstruct regional temperature history. The model is as follows:

$$T_{JAt} = 5.35I_{t+1} + 13.36, (r = 0.61, N = 58, R^2 = 37.1\%, R^2_{adj} = 36.9\%, F = 32.97, P < 0.001) \quad (1)$$

where T_{JAt} is RLST at year t and I_{t+1} is the ring width index at year $t+1$. The RLST reconstruction model accounted for 37.1% (36.9% after adjusting for the degrees of freedom) of the composite mean maximum temperature variance for calibration period from 1955 to 2012 (Fig. 4a, Table 2). Shown in Fig. 4a, our temperature reconstruction couldn't fully capture the magnitude of extraordinary warm or cold years at high frequency especially in the last few years similar to other tree-ring reconstructions (D'Arrigo et al., 1998), but it paralleled the general tendency of composite RLST during calibration period. Spatial correlation analysis showed a similar general pattern between the observed and estimated RLST compared with gridded temperature records (Fig. 5). These results suggest that our reconstructions provide some information about late summer mean maximum temperature variability for NWSP.

Split-period calibration/verification analysis (Cook and Kairiukstis, 1990;Fritts, 1976) was used to test the stability and reliability of the regression model including statistical parameters of r, R^2, RE, CE, ST, PMT, DW and RMSE. Two rigorous

Clim. Past Discuss., doi:10.5194/cp-2016-6, 2016
Manuscript under review for journal Clim. Past
Published: 3 February 2016

tests of fit, the RE and CE were both strongly positive (Table 2) indicating that the model was significantly and considerably skillful in reconstructing observed variations (Cook et al., 1999). The statistical parameters of R^2, ST and PMT all exceeded the 95% or 99% confidence level. The DW, used to analyze reconstruction residuals from a regression analysis, ranged from 1.68 to 1.99, indicating no significant autocorrelation or linear trends among our residuals (Table 2). Moreover, the RMSE value was relatively small in our model (Cook and Pederson, 2011). Upon successful validation of the two split-period models, regression parameters for the full calibration period were used to reconstruct RLST back to AD 1654 based on the ring-width record.

3.3 Regional temperature variations

According to the regression equation, our reconstructed RLST could be extended back to A.D. 1665 with a mean of 18.75 °C and a standard deviation (SD) of ±0.84°C (Fig. 4b). In this paper, we defined those having values (11-year moving average series) exceeding 19.58℃ (mean＋SD) as extremely warm periods, while those not exceeding 17.91℃ (mean－SD) as extremely cold periods. Relatively cold periods occurred during 1816-1821, 1836-1842, 1859-1869, 1878-1883, 1708-1711, 1765-1769, 1818-1821, 1824-1828, 1832-1836, 1839-1842 and 1869-1877. Warm periods prevailed during 1655-1668, 1719-1730 and 1858-1859. Among them, the ten coldest yeas were identified as 1872(16.49), 1764(16.55), 1766(16.68), 1874(16.94), 1707(17.01), 1932(17.05), 1680(17.1), 1770(17.1), 1705(17.15) and 1837(17.16), and the top ten warmest years were 1719(21.33), 1720(21.05), 1660(21.04), 1726(20.68), 1723(20.66), 1662(20.64), 1729(20.56), 1661(20.53),1911(20.52) and 1951(20.5), respectively.

During the period 1875–1955, late summer temperature fluctuated less strongly than before or thereafter. In general, the average length of cold periods was shorter than that of warm periods. The cold period of 1869-1877 was the longest and coldest cool period with a mean of 17.63 °C. The longest warm period extended from 1655 to 1668, while the warmest period in AD 1719-1730 with a mean of 20.37 °C. However, we should point out that the rapid warming during the 20th century wasn't extraordinary obvious in our reconstructed RLST.

A multitaper method (MTM) of spectral analysis (Mann and Lees, 1996) was performed to identify major periodicities present in the full range of our reconstruction. The result of spectral analysis over the full range (1665-2012) showed that there were significant periodicities at 2-2.3, 2.5, 3-3.1, 4.6-4.7, 5.6, 25-32 and 53-93 years at the 95% confidence level (Fig. 6).

4 Discussion

4.1 Climate-growth relationship

Temperature, especially winter or growing season temperature, limits tree growth at sub- and alpine treelines at high latitudes of Northern Hemisphere, as suggested by previous dendroclimatic and seasonal cambial activity studies (Körner and Paulsen, 2004;Wieser and Tausz, 2007;Seo et al., 2013;Rossi et al., 2008). Large temperature sensitivity, especially during the summer season, has also been clearly demonstrated in tree line sites of the eastern Tibetan Plateau (Fan et al., 2009;Zhu et al., 2011;Li

Clim. Past Discuss., doi:10.5194/cp-2016-6, 2016
Manuscript under review for journal Clim. Past
Published: 3 February 2016

et al., 2012). In our study, the radial growth of *P. purpurea* was significantly positive correlated to mean and maximum temperature in July and August of the previous year was also found, which suggests that previous late summer temperature was the major limiting factor to tree-ring growth of *P. purpurea* in NWSP, China (Fig. 3). Similar results show that the radial growth of *P. purpurea* was majorly limited by late summer temperature of previous and current years (Bräuning and Mantwill, 2004;Kang and Yang, 2013;Ren et al., 2014;Guo et al., 2015) and has been reported by previous studies in nearby areas; most of these have been used to reconstruct the historical temperature variations (Bräuning and Mantwill, 2004;Ren et al., 2014). Tree-ring chronologies are an indicator of late summer temperature, which was also found at high-elevation conifer sites on the eastern Tibetan Plateau (Bräuning, 2006;Bhattacharyya and Chaudhary, 2003;Bräuning and Mantwill, 2004), which further suggested that the growth of spruce trees in treelines of our study was greatly affected by previous late summer temperature. The lagged relationship to climate is common in dendroclimatology analyses (Li et al., 2012;Zhu et al., 2011;Gou et al., 2006;Duan et al., 2010;Bräuning and Mantwill, 2004), which usually involved the use of stored photosynthetic product during the current growing season and/or developmental processes (e.g. leaf maturation, root elongation) in the previous growing season (Fritts, 1976). It is possible that more non-structural carbohydrates (NSC) and other organic substances, which could be used to produce more wood in the next spring at high-elevation sites, were synthesized in a warmer late summer, although late wood would have formed and cambial activity would have stopped (Li et al., 2008). In contrast, by increasing the frequency of frost and missing rings and limiting the growth of roots and their function in water uptake (Körner and Paulsen, 2004), a narrow ring would usually be formed and less NSC and other organic substances would be synthesized in a cold late summer. Tree growth at timberlines not only depends on growing season temperature, but also occasionally on winter temperatures which could cause frost drought in evergreen conifers (Elliott, 2012;Mayr et al., 2006;Oberhuber, 2004). Generally, the radial growth of *P. purpurea* has a negative relationship with winter (from previous October to current April, especially in November) mean and minimum temperature rather than maximum temperature (Fig. 3). Warm winters often accompanied by low snow cover, which might particularly and likely lead trees to suffer from enhanced frost desiccation as a result of increased transpiration rates of needles and shoots, photoinhibitory stress and short-term fluctuations in shoot temperatures, leading to xylem embolism (Sperry and Robson, 2001;Havranek and Tranquillini, 1995). Sustained winter defoliation at tree line has an overwhelming influence on subsequent radial growth (Oberhuber, 2004;Payette et al., 1996). However, more snow protects plants against these stresses during the cold season (Sakai and Larcher, 1987). These explain negative correlation coefficients between mean minimum temperature in winter and *P. purpurea* growth at the tree line. Therefore, significant positive correlations of the radial growth of *P. purpurea* with the previous late summer mean and maximum temperature and positive correlation of the radial growth of *P. purpurea* and the previous winter mean minimum temperature were reasonable and meaningful in this study, based on inferences from known physiological processes.

4.2 Comparison with regional records

To assess whether our reconstruction represents features and evaluate the spatial synchrony of temperature variation, a spatial correlation analysis was performed between the 0.5º×0.5º gridded July-August mean maximum temperature data (CRU TS3.22;

Clim. Past Discuss., doi:10.5194/cp-2016-6, 2016
Manuscript under review for journal Clim. Past
Published: 3 February 2016

Harris et al., 2014) for the period 1955-2012 over a large region of NWSP. Both the observed and reconstructed late summer temperature for NWSP showed a similar spatial correlation pattern with regional temperature records, which was coherent over a large spatial scale, including most of the Tibetan Plateau, central and eastern regions of China, and parts of Mongolia and Inner Mongolia, China (Fig. 6). We also compared our reconstruction with other tree-ring based temperature reconstructions in surrounding regions (Fig. 7). The RLST variations for NWSP were coherent over a large spatial scale, again including most of the Tibetan Plateau, central and eastern regions of China, and parts of Mongolia and Inner Mongolia, China. July-August mean temperature, based on tree-ring data obtained nearby our study site, in the north of west Sichun of Xiao et al. (2015) was significantly positively (r = 0.122, p = 0.028) associated with our reconstruction (Fig. 7). Additionally, a significant positive correlation (r = 0.1, p = 0.039) between our reconstruction and February-June temperature reconstruction for Kathmandu (Cook et al., 2003), located farther from our study site, was also found (Fig. 7). Both the sites (farther and near our study site) displayed highly synchronous variation patterns with our reconstruction overall, which further validated results of spatial correlation analysis. However, there were some differences between them, which might be due to differences in season, species, as well as the different standardization approach applied on tree-ring data (Thapa et al. 2014). In addition, inherent differences in climate variables and in climate-driven mechanisms were also the main sources of differences. For example, variations of the mean, minimum, and maximum temperatures were often asymmetric (Wilson and Luckman, 2002;Wilson and Luckman, 2003;Gou et al., 2008). Asymmetric variability between mean, minimum and maximum temperatures was also found at the Hongyuan weather stations, especially the differences between mean minimum and maximum temperature.

It was noteworthy that 20th century warming (IPCC, 2013;Zhu et al., 2011;Song et al., 2007) was not very obvious in our reconstruction, which was in line with recent studies that global warming has occurred mainly in the minimum temperatures and at night in most regions of the Northern Hemisphere, however, evidence of the warming trend of the maximum temperatures was not clear (Wilson and Luckman, 2002;Wilson and Luckman, 2003). In short, our regional reconstruction could be a good representative of the past late summer maximum temperature variations of NWSP.

4.3 Possible forcing mechanism

Results of MTM analysis revealed that some significant dominant periodicities existed in our reconstructed regional temperature variability (Fig. 6). Among them, significant high-frequency periodicities around 5.7, 4.6–4.7, 3.0–3.1, 2.5 and 2.1–2.3 years, falling within the range of El Niño Southern Oscillation (ENSO) cycle of 2-8 years (Holton et al., 1989), were found in our reconstruction, which indicated that ENSO might affect the late summer temperature variability of NWSP. Consistent with this observation, ENSO may have a strong influence on temperature variability as has been reported in neighboring dendroclimatological research, such as northwest Yunnan (Fan et al., 2009;Li et al., 2011;Li et al., 2012), Tibetan Plateau (Bhattacharyya and Chaudhary, 2003;Bräuning and Mantwill, 2004;Gou et al., 2008;Gou et al., 2006;Zhu et al., 2011) and West Sichuan Plateau (Duan et al., 2010). Strong teleconnections of ENSO with interannual variability of tree growth and local temperature with tropical ocean-atmosphere systems has been found in nearby sites (Liang et al., 2008;Deng et al., 2014).

Clim. Past Discuss., doi:10.5194/cp-2016-6, 2016
Manuscript under review for journal Clim. Past
Published: 3 February 2016

Based on these results we performed correlation analysis of the smoothed (11-yr moving averaged) temperature series with extended Multivariate ENSO Index (MEI, Wolter and Timlin, 2011). A significant negative correlation was found between estimated RLST and MEI from the previous May to current August (Table 3) revealing that the cool (warm) previous and current SSTs might have a significant impact on late summer temperature over the NWSP. Similar results were detected over the western Nepal Himalaya region (Thapa et al., 2014) and Northern China (Lu, 2005). These high-frequency cycles around 2–3 year might also linked to the quasi-biennial oscillation (QBO, Labitzke and Van Loon, 1999) and tropospheric biennial oscillation (TBO, Meehl, 1987), which may also suggest strong teleconnections of local temperature variability with tropical ocean-atmosphere systems.

The significant cycle around 25–32 years might be linked to Pacific Decadal Oscillation (PDO, Mantua et al., 1997), and significantly negative correlations of our smoothed (11-yr moving averaged) temperature reconstruction with PDO index from the previous May to current August were also detected (Table 3). This result coincides with the fact that PDO signals could be found in tree rings over large-scale Asian regions (D'Arrigo and Wilson, 2006). Accompanied by significant peaks at 60.2- and 73-years, the continuously periodicities around 49-114 years in our regional temperature reconstruction might tentatively be related to PDO, Atlantic Multidecadal Oscillation (AMO, Enfield et al., 2001) as well as solar activity (Peristykh and Damon, 2003;Raspopov et al., 2004;Shindell et al., 1999;Eddy, 1976;Braun et al., 2005). The AMO was an important driver of multidecadal variations in summer climate not only in North America and Western Europe (Sutton and Hodson, 2005;Kerr, 2000), but also in the East Asian (Zhu et al., 2011;Wang et al., 2011;Feng and Hu, 2008;Wang et al., 2015;Liang et al., 2008). The 60.2-year peak associated with AMO demonstrated that multidecadal variations of late summer temperature of NWSP might be controlled by AMO. This was also consistent with recent findings; the AMO could change the land-sea thermal contrast between the East Asian continents thus affecting temperature of the East Asian (Wang et al., 2011;Feng and Hu, 2008;Li and Yanai, 1996). Further, correlation analysis between the smoothed (11-yr moving averaged) temperature reconstruction and the monthly AMO index was calculated to test this hypothesis. A significant negative correlation during the previous July to September period and current May to August period was detected (Table 3), which further evidenced the powerful influence of AMO on late summer temperatures in northwest Sichuan. In addition, we also found significant cycles at more than 147 years with peaks at 170 years. Considering the limited length of our reconstruction (368 yrs), this cycle might not be reliable and must be interpreted with caution, although there have been similar findings using temperature reconstruction for the Eastern (Wang et al., 2015), north eastern (Liu et al., 2011) and south eastern (Deng et al., 2014) Tibetan Plateau.

Solar activity associated with regional temperatures of northwest Sichuan, even the classic 11-yr sunspot cycle (Shindell et al., 1999), was not significant in our temperature reconstruction. However, those significant multidecadal and centennial-scale cycles of our temperature reconstruction might also include the signs of solar activity, such as the Gleissberg cycles (Peristykh and Damon, 2003), Suess cycles (Braun et al., 2005), Bruckner cycles (Raspopov et al., 2004) and Schwabe cycles (Braun et al., 2005). The Maunder (circa AD 1645–1715) and Dalton (circa AD 1790–1820) solar minima periods were generally associated with temperature depressions (Eddy, 1976), and the Damon (circa AD 1890–1920) solar maximum period occurred

Clim. Past Discuss., doi:10.5194/cp-2016-6, 2016
Manuscript under review for journal Clim. Past
Published: 3 February 2016

in a relatively warm period, which further confirmed that late summer temperature variation of NSWP might be driven by solar activity.

5 Conclusion

In this study, a high resolution tree-ring chronology was used to reconstruct RLST of NWSP from 1645 to 2012. The model of our reconstruction explains 37.1 % of the variance during the common period 1955–2012. Cold periods occurred in AD 1816–1821, 1836–1842, 1859–1869, 1878–1883, 1708-1711, 1765-1769, 1818-1821, 1824-1828, 1832-1836, 1839-1842 and 1869-1877, and warm periods occurred in AD 1655-1668, 1719-1730 and 1858-1859. Spatial correlations with gridded land mean maximum temperature data and comparison with other nearby temperature reconstructions further revealed that the RLST has high spatial representativeness. 20th century rapid warming wasn't obvious in our RLST reconstruction, which implies that mean maximum temperature, as a unique temperature indicator, might play an important and different role in global change. Spectral analysis of our reconstruction revealed significant quasi-cycles of 169-, 147-, 49-114-, 25–32-, 5.7-, 4.6–4.7-, 3.0–3.1-, 2.5- and 2.1–2.3-years at a 95% confidence level. The mean maximum temperature variability in NWSP might be linked with ENSO, PDO, AMO and solar activity.

Acknowledgements This research was supported by the National Natural Science Foundation of China (Nos. 31370463 and 41471168), the Program for New Century Excellent Talents in University (NCET-12-0810), and the Program for Changjiang Scholars and Innovative Research Team in University (IRT-15R09). We would like to thank Alison Beamish at the University of British Columbia for her assistance with English language and grammatical editing of the manuscript. We also thank the staff of Aba Forestry Bureaus for their assistance in the field.

References

Bhattacharyya, A., and Chaudhary, V.: Late-summer temperature reconstruction of the eastern Himalayan region based on tree-ring data of Abies densa, Arctic, Antarctic, and Alpine Research, 35, 196-202, 2003.

Bräuning, A., and Mantwill, B.: Summer temperature and summer monsoon history on the Tibetan plateau during the last 400 years recorded by tree rings, Geophysical Research Letters, 31, 2004.

Bräuning, A.: Tree-ring evidence of 'Little Ice Age'glacier advances in southern Tibet, The Holocene, 16, 369-380, 2006.

Braun, H., Christl, M., Rahmstorf, S., Ganopolski, A., Mangini, A., Kubatzki, C., Roth, K., and Kromer, B.: Possible solar origin of the 1,470-year glacial climate cycle demonstrated in a coupled model, Nature, 438, 208-211, 2005.

Briffa, K. R., Jones, P. D., Schweingruber, F. H., Shiyatov, S. G., and Cook, E. R.: Unusual twentieth-century summer warmth in a 1,000-year temperature record from Siberia, Nature, 376, 156-159, 1995.

Cook, E. R.: A Time Series Analysis Approach to Tree Ring Standardization, University of Arizona, Arizona,USA, 1985.

Cook, E. R., and Kairiukstis, L. A.: Methods of dendrochronology: applications in the environmental sciences, Springer

Science & Business Media, 1990.

Cook, E. R., Meko, D. M., Stahle, D. W., and Cleaveland, M. K.: Drought reconstructions for the continental United States, Journal of Climate, 12, 1145-1162, 1999.

Cook, E. R., Krusic, P. J., and Jones, P. D.: Dendroclimatic signals in long tree-ring chronologies from the Himalayas of Nepal, International Journal of Climatology, 23, 707-732, 2003.

Cook, E. R., and Pederson, N.: Uncertainty, emergence, and statistics in dendrochronology, in: Dendroclimatology, Springer, 77-112, 2011.

D'Arrigo, R., and Wilson, R.: On the Asian expression of the PDO, International Journal of Climatology, 26, 1607-1618, 2006.

D'Arrigo, R., Cook, E., Salinger, M., Palmer, J., Krusic, P., Buckley, B., and Villalba, R.: Tree-ring records from New Zealand: long-term context for recent warming trend, Climate Dynamics, 14, 191-199, 1998.

Deng, Y., Gou, X., Gao, L., Yang, T., and Yang, M.: Early-summer temperature variations over the past 563yr inferred from tree rings in the Shaluli Mountains, southeastern Tibet Plateau, Quaternary Research, 81, 513-519, 2014.

Duan, J., Wang, L., Li, L., and Chen, K.: Temperature variability since AD 1837 inferred from tree-ring maximum density of Abies fabri on Gongga Mountain, China, Chinese Science Bulletin, 55, 3015-3022, 2010.

Eddy, J. A.: The maunder minimum, publisher not identified, 1976.

Elliott, G. P.: Extrinsic regime shifts drive abrupt changes in regeneration dynamics at upper treeline in the Rocky Mountains, USA, Ecology, 93, 1614-1625, 2012.

Fan, Z.-X., Bräuning, A., Yang, B., and Cao, K.-F.: Tree ring density-based summer temperature reconstruction for the central Hengduan Mountains in southern China, Global and Planetary Change, 65, 1-11, 2009.

Feng, S., and Hu, Q.: How the North Atlantic Multidecadal Oscillation may have influenced the Indian summer monsoon during the past two millennia, Geophysical Research Letters, 35, 2008.

Fritts, H. C.: Tree rings and climate, Elsevier, 1976.

Gou, X.-H., Yang, M., Peng, J.-F., Zhang, Y., Chen, T., and Hou, Z.-D.: Maximum temperature reconstruction for Animaqing Mountains over past 830 years based on tree ring records, Quaternary Sciences, 26, 991-998, 2006.

Gou, X., Chen, F., Yang, M., Gordon, J., Fang, K., Tian, Q., and Zhang, Y.: Asymmetric variability between maximum and minimum temperatures in Northeastern Tibetan Plateau: evidence from tree rings, Science in China Series D: Earth Sciences, 51, 41-55, 2008.

Guo, M., Zhang, Y., Wang, X., and Liu, S.: Difference in responses of major tree species growth to climate in the Miyaluo Mountains, western Sichuan, China, Chinese Journal of Applied Ecology, 26, 2237-2243, 2015.

Havranek, W. M., and Tranquillini, W.: Physiological processes during winter dormancy and their ecological significance, Ecophysiology of coniferous forests, 95-124, 1995.

Holmes, R. L.: Computer-assisted quality control in tree-ring dating and measurement, Tree-ring bulletin, 43, 69-78, 1983.

Holton, J. R., Dmowska, R., and Philander, S. G.: El Niño, La Niña, and the southern oscillation, Academic press, 1989.

IPCC: Climate change 2013: the physical science basis. Contribution of working group I to the fifth assessment report of the

intergovernmental panel on climate change, Cambridge, 2013.

Körner, C., and Paulsen, J.: A world-wide study of high altitude treeline temperatures, Journal of Biogeography, 31, 713-732, 2004.

Kang, S., and Yang, B.: The response of tree-ring growth of *Picea purpurea* and *Picea crassifolia* in South Gansu province to climate change, J Desert Res, 2, 619-625, 2013.

Kerr, R. A.: A North Atlantic climate pacemaker for the centuries, Science, 288, 1984-1985, 2000.

Li, C., and Yanai, M.: The onset and interannual variability of the Asian summer monsoon in relation to land-sea thermal contrast, Journal of Climate, 9, 358-375, 1996.

Li, M., Xiao, W., Shi, P., Wang, S., Zhong, Y., Liu, X., Wang, X., Cai, X., and Shi, Z.: Nitrogen and carbon source–sink relationships in trees at the Himalayan treelines compared with lower elevations, Plant, cell & environment, 31, 1377-1387, 2008.

Li, Q.: Sichuan soil, Sichuan Publishing House of Science & Technology, Chendu, China, 1995.

Li, Z., Shi, C. M., Liu, Y., Zhang, J., Zhang, Q., and Ma, K.: Summer mean temperature variation from 1710-2005 inferred from tree-ring data of the Baimang Snow Mountains, northwestern Yunnan, China, Climate Research, 47, 207, 2011.

Li, Z., Zhang, Q., and Ma, K.: Tree-ring reconstruction of summer temperature for AD 1475–2003 in the central Hengduan Mountains, Northwestern Yunnan, China, Climatic Change, 110, 455-467, 2012.

Liang, E., Shao, X., and Qin, N.: Tree-ring based summer temperature reconstruction for the source region of the Yangtze River on the Tibetan Plateau, Global and Planetary Change, 61, 313-320, 2008.

Liu, J., Yang, B., and Qin, C.: Tree-ring based annual precipitation reconstruction since AD 1480 in south central Tibet, Quaternary International, 236, 75-81, 2011.

Lu, R.: Interannual variation of North China rainfall in rainy season and SSTs in the equatorial eastern Pacific, Chinese Science Bulletin, 50, 2069-2073, 2005.

Ma, L.: China Meteorological Disaster Authority (Sichuan Volume), Meteorological Press, Beijing, China, 2006.

Mann, M. E., and Lees, J. M.: Robust estimation of background noise and signal detection in climatic time series, Climatic change, 33, 409-445, 1996.

Mayr, S., Hacke, U., Schmid, P., Schwienbacher, F., and Gruber, A.: Frost drought in conifers at the alpine timberline: xylem dysfunction and adaptations, Ecology, 87, 3175-3185, 2006.

Oberhuber, W.: Influence of climate on radial growth of Pinus cembra within the alpine timberline ecotone, Tree physiology, 24, 291-301, 2004.

Payette, S., Delwalde, A., Morneau, C., and Lavole, C.: Patterns of tree stem decline along a snow-drift gradient at treeline: a case study using stem analysis, Canadian Journal of Botany, 74, 1671-1683, 1996.

Peristykh, A. N., and Damon, P. E.: Persistence of the Gleissberg 88‐year solar cycle over the last~ 12,000 years: Evidence from cosmogenic isotopes, Journal of Geophysical Research: Space Physics (1978–2012), 108, SSH 1-1-SSH 1-15, 2003.

Qin, N., Shi, X., Shao, X., and Wang, Q.: Average maximum temperature change recorded by tree rings in west Sichuan Plateau,

Plateau and Mountain Meteorology Research, 28, 18-24, 2008.

Raspopov, O., Dergachev, V., and Kolström, T.: Periodicity of climate conditions and solar variability derived from dendrochronological and other palaeoclimatic data in high latitudes, Palaeogeography, Palaeoclimatology, Palaeoecology, 209, 127-139, 2004.

Ren, J., Liu, Y., Song, H., Ma, Y., Li, Q., Wang, Y., and Cai, Q.: The historical reconstruction of the maximum temperature over the past 195 years, Linxia region, Gansu Provincce—Based on the data from *Picea purpurea* Mast., Quaternary Sciences, 34, 1270-1279, 2014.

Rossi, S., Deslauriers, A., Griçar, J., Seo, J. W., Rathgeber, C. B., Anfodillo, T., Morin, H., Levanic, T., Oven, P., and Jalkanen, R.: Critical temperatures for xylogenesis in conifers of cold climates, Global Ecology and Biogeography, 17, 696-707, 2008.

Sakai, A., and Larcher, W.: Frost survival of plants. Responses and adaptation to freezing stress, Springer-Verlag, 1987.

Seo, J.-W., Eckstein, D., Olbrich, A., Jalkanen, R., Salminen, H., Schmitt, U., and Fromm, J.: Climate control of wood formation: illustrated for Scots pine at its northern distribution limit, in: Cellular Aspects of Wood Formation, Springer, 159-185, 2013.

Shao, X., and Fan, J.: Past climate on west Sichuan Plateau as reconstructed from ring-widths of dragon spruce, Quaternary Sciences, 1, 81-89, 1999.

Shindell, D., Rind, D., Balachandran, N., Lean, J., and Lonergan, P.: Solar cycle variability, ozone, and climate, Science, 284, 305-308, 1999.

Song, H., Liu, Y., Ni, W., Cai, Q., Sun, J., Ge, W., and Xiao, W.: Winter mean lowest temperature derived from tree-ring width in Jiuzhaigou region, China since 1750 AD, Quaternary Sciences, 27, 486-491, 2007.

Sperry, J. S., and Robson, D. J.: Xylem cavitation and freezing in conifers, in: Conifer cold hardiness, Springer, 121-136, 2001.

Stokes, M. A., and Smiley, T. L.: An introduction to tree-ring dating, University of Arizona Press, Arizona, USA, 1968.

Sutton, R. T., and Hodson, D. L.: Atlantic Ocean forcing of North American and European summer climate, Science, 309, 115-118, 2005.

Thapa, U. K., Shah, S. K., Gaire, N. P., and Bhuju, D. R.: Spring temperatures in the far-western Nepal Himalaya since AD 1640 reconstructed from Picea smithiana tree-ring widths, Climate Dynamics, 1-13, 2014.

Wang, J., Yang, B., and Ljungqvist, F. C.: A Millennial Summer Temperature Reconstruction for the Eastern Tibetan Plateau from Tree Ring Width, Journal of Climate, 2015.

Wang, X., Brown, P. M., Zhang, Y., and Song, L.: Imprint of the Atlantic multidecadal oscillation on tree-ring widths in Northeastern Asia since 1568, PloS one, 6, e22740, 2011.

Wieser, G., and Tausz, M.: Trees at their upper limit: treelife limitation at the alpine timberline, Springer Science & Business Media, 2007.

Wigley, T. M., Briffa, K. R., and Jones, P. D.: On the average value of correlated time series, with applications in dendroclimatology and hydrometeorology, Journal of climate and Applied Meteorology, 23, 201-213, 1984.

Wilson, R. J., and Luckman, B. H.: Tree-ring reconstruction of maximum and minimum temperatures and the diurnal

temperature range in British Columbia, Canada, Dendrochronologia, 20, 257-268, 2002.

Wilson, R. J., and Luckman, B. H.: Dendroclimatic reconstruction of maximum summer temperatures from upper treeline sites in Interior British Columbia, Canada, The Holocene, 13, 851-861, 2003.

Wu, P., Wang, L., and Shao, X.: Reconstruction of summer temperature from maximum latewood density of Pinus densata in West Sichuan, Acta Geographica Sinica, 60, 998-991, 2005.

Xiao, D., Qin, N., Li, J., and Li, Y.: Change of Mean Maximum Temperature in July during 1506-2008 in Seda of West Sichuan Plateau According to Reconstructed Tree-ring Series, Journal of Desert Research, 33, 1536-1543, 2013.

Xiao, D., Qin, N., and Huang, X.: A 325-year reconstruction of July-August mean temperature in the north of west Sichun derived from tree-ring, Quaternary Sciences, 2015.

Yang, Y., Li, C., and Guan, Z.: Sichuan Forest, China Forestry Publishing House, Beijing, China, 1992.

Yu, S., Yuan, Y., Wei, W., Zhang, T., Shang, H., and Chen, F.: Reconstructed mean temperature in Mearkang, West Sichuan in July and its detection of climatic period signal, Plateau Meteorol, 31, 193-200, 2012.

Zhang, Z. H.: Tree-rings, a key ecological indicator of environment and climate change, Ecological Indicators, 51, 107-116, 2015.

Zheng, D., and Yao, T.: Uplifting of Tibetan Plateau with its environmental effects, SciencePress, Beijing, 2004.

Zhu, H., Shao, X., Yin, Z., and Huang, L.: Early summer temperature reconstruction in the eastern Tibetan Plateau since AD 1440 using tree-ring width of Sabina tibetica, Theoretical and Applied Climatology, 106, 45-53, 2011.

Clim. Past Discuss., doi:10.5194/cp-2016-6, 2016
Manuscript under review for journal Clim. Past
Published: 3 February 2016

Climate of the Past Discussions
Open Access
EGU

Tables

Table 1 Information on the two weather stations sites nearest to sampling sites.

Weather stations	Hongyuan	Aba
Long. (E)	102°33′	101°41′
Lat. (N)	32°48′	32°54′
Elev. (m)	3248	3254
P (mm)	749.89	740.77
T (℃)	1.53	3.43
Tmax (℃)	10.24	12.22
Tmin (℃)	-5.35	-2.93
Period	1960-2013	1955-1990
DWS (km)	42.4	42.3

Note: P is annual total precipitation. T, T*max* and T*min* are annual mean, maximum and minimum temperature, respectively. DWS is the distance from weather station to the sampling site of Chali.

Table 2 Calibration and verification statistics for the regional Jul-Aug mean maximum temperature reconstruction

Calibration	*r*	R^2	Verification	R^2	RE	CE	ST	PMT	DW	RMSE
1955-2012	0.61**	0.37**	—	—	0.37	—	(41,17)**	6.46**	1.68	0.73
1955-1984	0.78**	0.61**	1985-2012	0.28**	0.26	0.21	(21,8)*	4.04**	1.99	0.82
1985-2012	0.53**	0.28**	1955-1984	0.61**	0.61	0.59	(24,5)**	4.63**	1.69	0.62

* = $p < 0.05$, ** = $p < 0.01$.

Clim. Past Discuss., doi:10.5194/cp-2016-6, 2016
Manuscript under review for journal Clim. Past
Published: 3 February 2016

Climate of the Past Discussions
Open Access
EGU

Table 3 Correlation of the smoothed (11-yr moving averaged) temperature reconstruction and other large-scale climate system cycles.

Month	AMO (n=156)	PDO (n=112)	MEI (n=62)
PMAY	-0.15	-0.43**	-0.43**
PJUN	-0.19*	-0.26**	-0.42**
PJUL	-0.19*	-0.27**	-0.32*
PAUG	-0.17*	-0.27**	-0.27*
PSEP	-0.17*	-0.24*	-0.27*
POCT	-0.07	-0.19*	-0.288*
PNOV	-0.05	-0.21*	-0.26*
PDEC	-0.07	-0.21*	-0.28*
JAN	-0.00	-0.34**	-0.28*
FEB	-0.13	-0.29**	-0.27*
MAR	-0.13	-0.39**	-0.38**
APR	-0.13	-0.39**	-0.41**
MAY	-0.18*	-0.46**	-0.43**
JUN	-0.22**	-0.31**	-0.42**
JUL	-0.22**	-0.30**	-0.31*
AUG	-0.21**	-0.30**	-0.28*

AMO: Atlantic Multidecadal Oscillation; PDO: Pacific Decadal Oscillation; MEI: Multivariate ENSO Index

* $p < 0.05$, ** $p < 0.01$

Clim. Past Discuss., doi:10.5194/cp-2016-6, 2016
Manuscript under review for journal Clim. Past
Published: 3 February 2016

Climate of the Past Discussions
Open Access
EGU

Figures

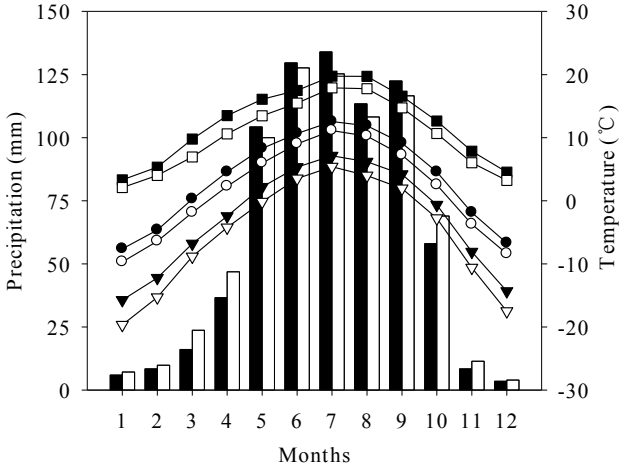

15 **Fig. 1** Monthly variation of total precipitations (bars), mean maximum temperature (line with squares), mean temperature (line with circles), and mean minimum temperature (line with triangles) for Hongyuan (filled with white) and Aba (filled with black) meteorological stations, calculated for the period of 1961–2013 and 1955–1990, respectively.

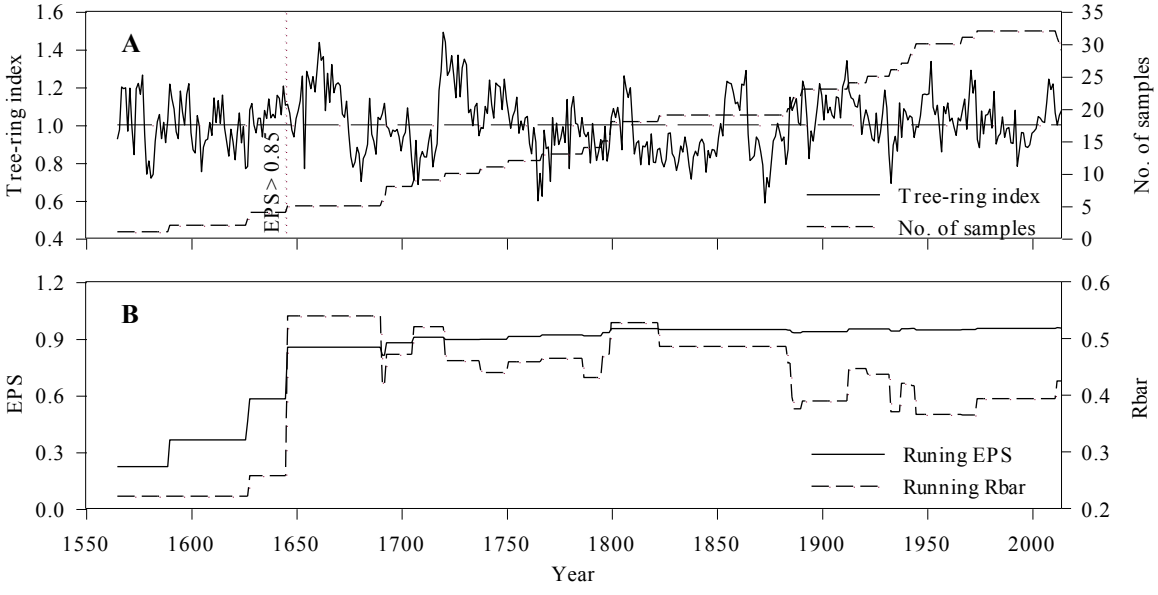

Clim. Past Discuss., doi:10.5194/cp-2016-6, 2016
Manuscript under review for journal Clim. Past
Published: 3 February 2016

Climate of the Past Discussions
Open Access
EGU

Fig. 2 The tree-ring chronology of timberline *Picea purpurea* in Chali. A, Standard chronology and changing sample size over time and B, Running EPS and Rbar.

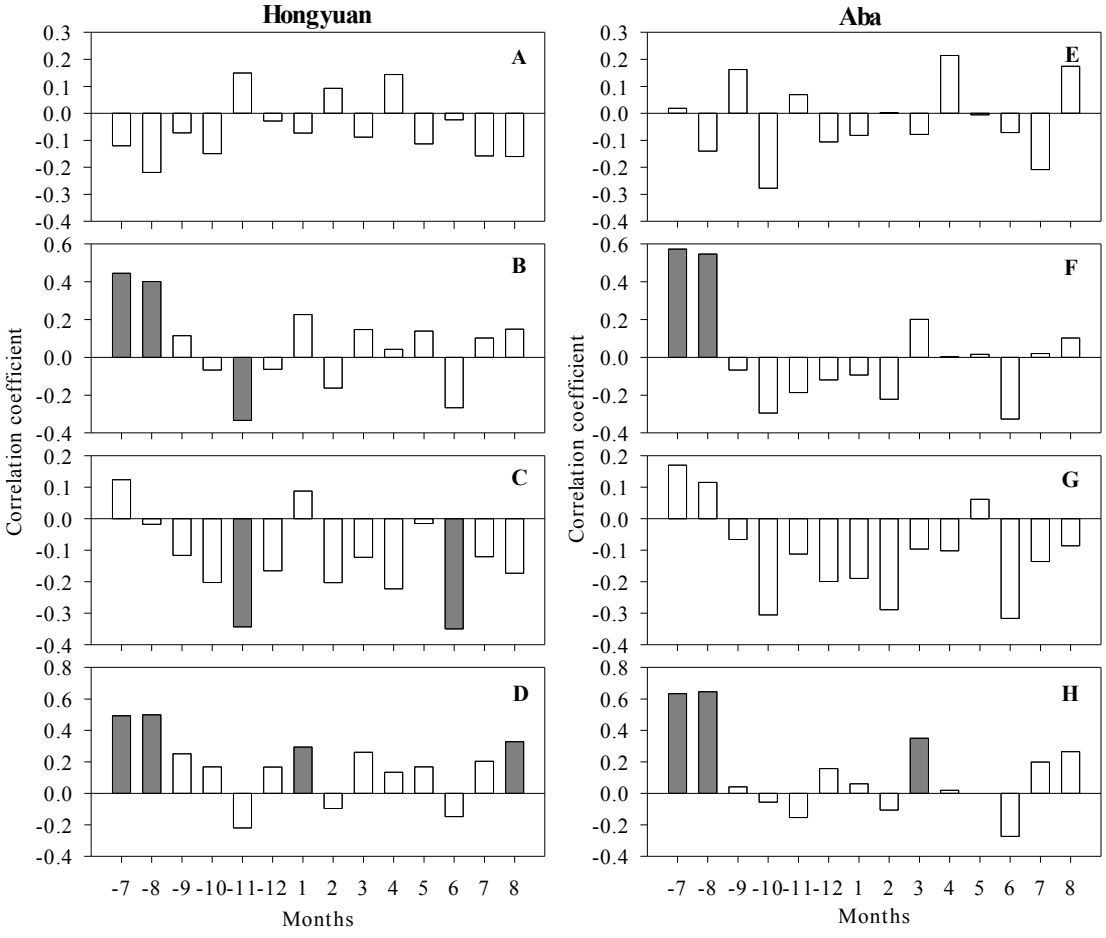

Fig. 3 Correlation analyses between the Chali tree-ring chronology and meteorological climate data of Hongyuan and Aba including mean total precipitation (A, E), mean temperature (B, F), minimum temperature(C, G), and maximum temperature (D, H). The gray-filled bars represent significant effects at 95 % significant levels.

Clim. Past Discuss., doi:10.5194/cp-2016-6, 2016
Manuscript under review for journal Clim. Past
Published: 3 February 2016

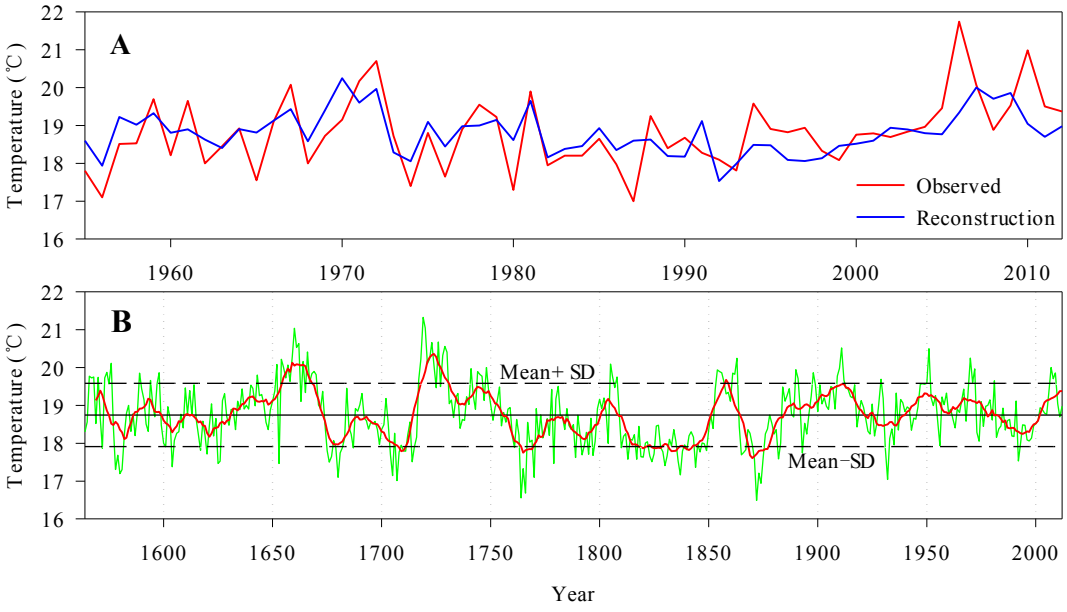

Fig. 4 Temperature reconstruction for NWSP, China. A, The comparison of observed and reconstructed regional Jul-Aug mean maximum temperature during the calibration period 1955-2012; B, Tree-ring reconstruction of regional Jul-Aug mean maximum temperature, plotted annually from 1564 to 2012 (cyan line), along with a smoothed 11-year moving average (red line).

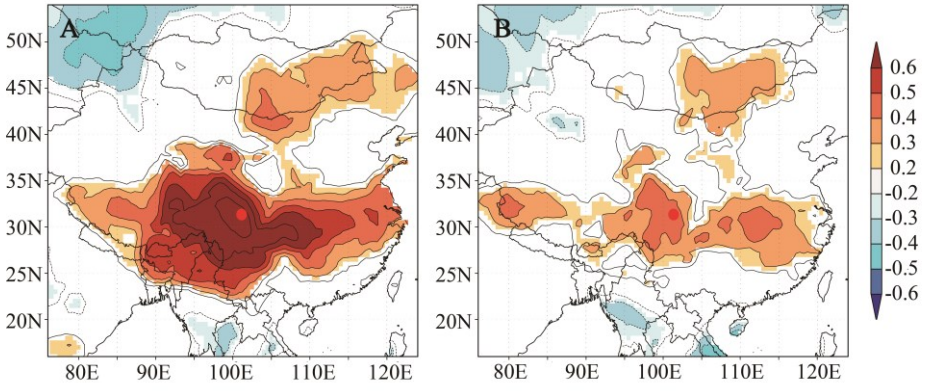

Fig. 5 Spatial correlation fields of (A) instrumental and (B) reconstructed July-August mean maximum temperature for NWSP with regional gridded July-August mean maximum temperature for the period 1955–2011.

Clim. Past Discuss., doi:10.5194/cp-2016-6, 2016
Manuscript under review for journal Clim. Past
Published: 3 February 2016

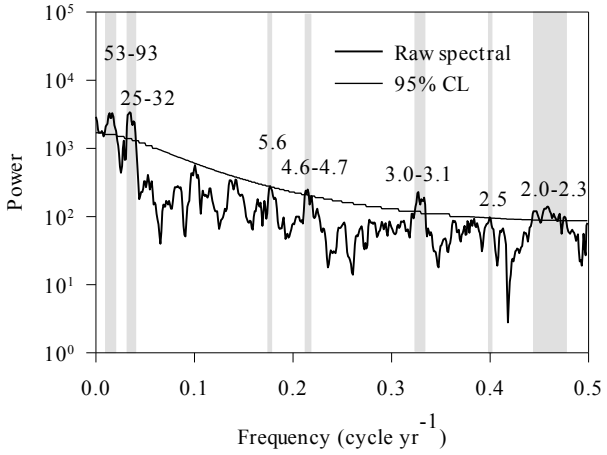

Fig. 6 Multi-taper method power spectrum of the reconstructed July-August temperature for the period AD 1645-2012. The 95% and 99% confidence level relative to red noise is shown by the dashed curve. The gray area indicates the 95% significance level and the numbers refer to the significant period in years.

Clim. Past Discuss., doi:10.5194/cp-2016-6, 2016
Manuscript under review for journal Clim. Past
Published: 3 February 2016

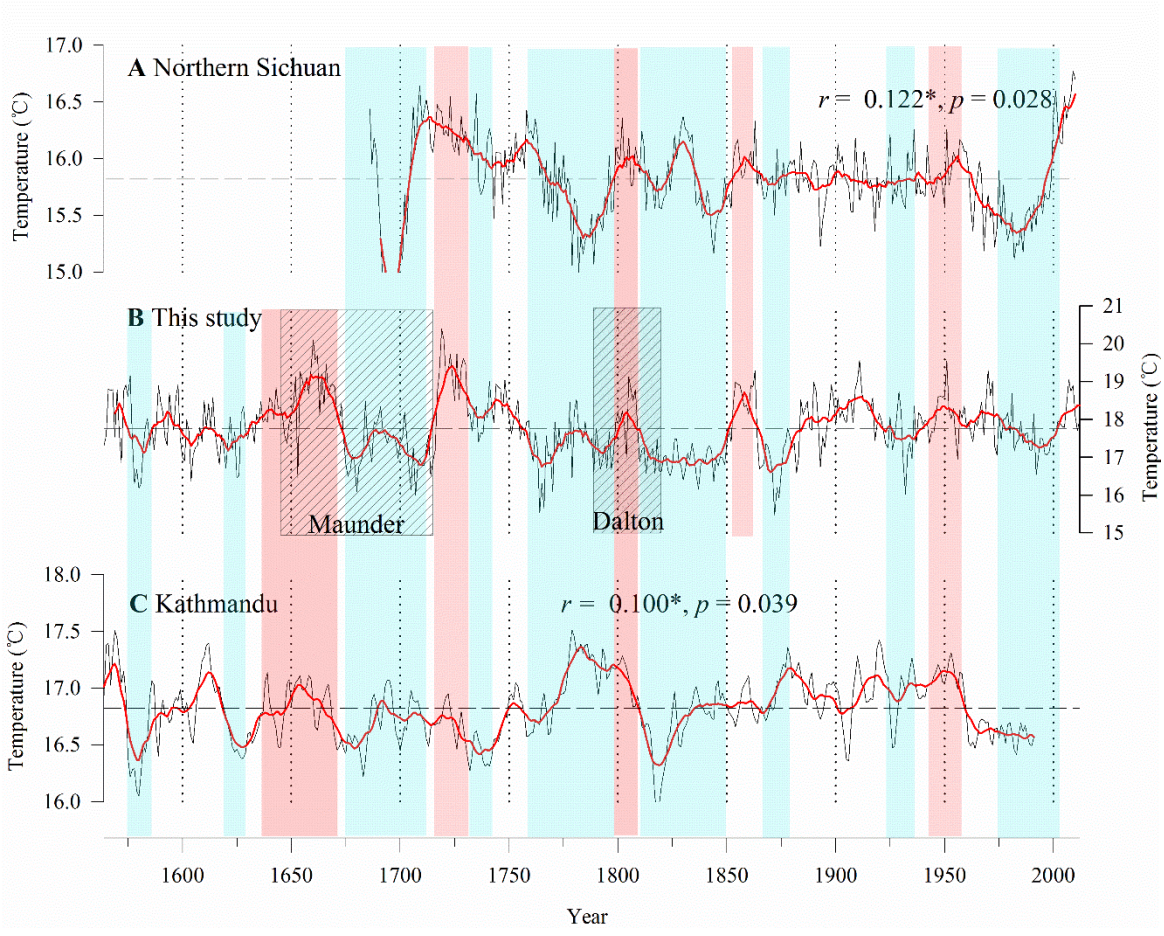

Fig. 7 Comparison of July-August mean maximum temperature reconstruction of NWSP in this study with other tree-ring based temperature reconstructions. A July-August mean temperature in northwest Sichun (Xiao et al., 2015), B July-August mean maximum temperature reconstruction for NWSP (this study), and C February-June temperature reconstruction for Kathmandu (Cook et al., 2003). All series are smoothed with an 11-year moving average (red curve). Blue (cold) and red (warm) shading are low and high temperature zones with good agreements in these temperature series, respectively.